Natural convection from a body to its spherical enclosure
by Charles Timothy McCoy

A thesis submitted to the Graduate Faculty in partial fulfillment of the requirements for the degree of
MASTER OF SCIENCE in Mechanical Engineering
Montana State University

Abstract:
An analysis of the heat transfer results and temperature profiles obtained experiment ally in a finite natural convection environment are presented and discussed. Overall heat transfer correlations for a cylinder and a cube located concentrically within a spherical enclosure were formulated using several test fluids yielding a wide range of the important parameters. These parameters include the Prandtl number, Rayleigh number, and a ratio of characteristic lengths describing the test geometry under investigation.

A Prandtl number effect on the convective heat transfer was noted for the cylinder study. Increasing viscosity and low ratios of overall cylinder length to cylinder diameter appeared to damp out the geometric effect inherent to the cylindrical body compared to a sphere.

The cube study indicated a very slight Prandtl number effect.

For this geometry, the heat transfer results could be correlated in terms of a Nusselt number as a function of a Rayleigh number and a geometric parameter only.

Possible flow patterns existing in the gap were deduced from the temperature profiles for both the cylinder and cube inner bodies.

Five characteristic regions were generally inherent to all temperature profiles. A multicellular flow was postulated to exist to explain exceptions to the general shape of the temperature profiles for both the cube and cylinder investigations.

Statement of Permission to Copy

In presenting this thesis in partial fulfillment of the requirements for an advanced degree at Montana State University, I agree that the Library shall make it freely available for inspection. I further agree that permission for extensive copying of this thesis for scholarly purposes may be granted by my major professor, or, in his absence, by the Director of Libraries. It is understood that any copying or publication of this thesis for financial gain shall not be allowed without my written permission.

Signature Charles T. McCoy

Date Sept. 13, 1972

NATURAL CONVECTION FROM A BODY TO ITS SPHERICAL ENCLOSURE

by

CHARLES TIMOTHY McCOY

A thesis submitted to the Graduate Faculty in partial fulfillment of the requirements for the degree

of

MASTER OF SCIENCE

in

Mechanical Engineering

Approved:

E. A. Bishop
Head, Major Department

Ralph C. Powe
Chairman, Examining Committee

Henry L. Parsons
Graduate Dean

MONTANA STATE UNIVERSITY
Bozeman, Montana

December, 1972

ACKNOWLEDGMENT

The author wishes to express his sincere thanks and appreciation to Dr. R. E. Powe, Dr. E. H. Bishop, and Dr. J. A. Scanlan for their advice and guidance. Thanks are also due Gordon Williamson who constructed the apparatus. The writer is especially appreciative of the patience and understanding of his wife, Donna.

The work reported in this thesis was supported by the Atomic Energy Commission under Contract Number AT(45-1)-2214.

TABLE OF CONTENTS

LIST OF TABLES

LIST OF FIGURES

ABSTRACT

An analysis of the heat transfer results and temperature profiles obtained experimentally in a finite natural convection environment are presented and discussed. Overall heat transfer correlations for a cylinder and a cube located concentrically within a spherical enclosure were formulated using several test fluids yielding a wide range of the important parameters. These parameters include the Prandtl number, Rayleigh number, and a ratio of characteristic lengths describing the test geometry under investigation.

A Prandtl number effect on the convective heat transfer was noted for the cylinder study. Increasing viscosity and low ratios of overall cylinder length to cylinder diameter appeared to damp out the geometric effect inherent to the cylindrical body compared to a sphere.

The cube study indicated a very slight Prandtl number effect. For this geometry, the heat transfer results could be correlated in terms of a Nusselt number as a function of a Rayleigh number and a geometric parameter only.

Possible flow patterns existing in the gap were deduced from the temperature profiles for both the cylinder and cube inner bodies. Five characteristic regions were generally inherent to all temperature profiles. A multicellular flow was postulated to exist to explain exceptions to the general shape of the temperature profiles for both the cube and cylinder investigations.

NOMENCLATURE

Symbol	Description
a, b	Characteristic lengths
A	Area
A_s	Surface area of inner body
C_p	Specific heat
C_1, C_2, C_3, C_4, C_5	Empirical constants
F	Denotes function
Gr_a	Grashof number, $g\beta\rho^2 a^3 \Delta T/\mu^2$
g	Acceleration of gravity
h	Length of vertical section of cylinder
H	Overall length of cylinder, $h + 2r_i$
$\bar{h}$	Average heat transfer coefficient for inner body, $q_c/A_s \Delta T$
I	Current through heaters located in inner body
k	Thermal conductivity
k_{eff}	Effective thermal conductivity
l_c	Length of cube side
L	Gap width, $r_o - r_i$
$\bar{L}$	Dimensionless length ratio
Nu_a	Nusselt number, $\bar{h}\, a/k$
Nu*	Modified Nusselt number defined by equation (1.5)
Pr	Prandtl number, $\mu C_p/k$

Symbol	Description
q_c	Heat transferred by convection
q_{cond}	Heat transferred by conduction down supporting stem
q_L	Heat loss by system
r_a	Average radius, $(r_o + r_i)/2$
r_i	Inner body radius or $l_c/2$
r_o	Outer body radius
r_θ	Distance from geometric center to a selected location on surface of inner body
$\overline{R}$	Dimensionless radius ratio, $(r - r_\theta)/(r_o - r_\theta)$
Ra_a	Rayleigh number, Gr_a Pr
Ra*	Modified Rayleigh number, Ra_L (L/r_i)
T	Temperature
$\overline{T}$	Dimensionless temperature, $(T - T_o)/(T_i - T_o)$
T_{am}	Arithmetic-mean temperature, $(T_i + T_o)/2$
T_i	Inner body temperature
T_m	Volumetric-mean temperature defined by equation (1.3)
T_o	Outer body temperature
V	Voltage across heaters located in inner body
β	Thermal expansion coefficient
ΔT	Temperature difference, $(T_i - T_o)$
ΔX	Distance

Symbol	Description
μ	Dynamic viscosity
ρ	Density
ϕ	Angular position measured from upward vertical axis.

CHAPTER I

INTRODUCTION

The analytical study of natural convection heat transfer occurring within finite enclosures is very difficult even when working with relatively simple geometries. This results from the governing equations describing the energy and flow fields being coupled and nonlinear. The boundary conditions inherent to each heat transfer system adds to the complexity of an analytical solution in many cases. Since many engineering systems involving natural convection heat transfer within a finite boundary do not lend themselves to an analytical analysis, other methods must be used for the prediction of the heat transfer phenomena occurring. One such method is an experimental investigation.

The objective of this investigation is to experimentally study natural convection heat transfer between either a cylinder or a cube and its spherical enclosure. This study is an extension of past work.

As shown in many publications discussing natural convection within finite enclosures, non-dimensionalizing the governing equations show that the heat transfer can be formulated in the following manner:

$$Nu_a = F\,[Gr_a,\ Pr,\ \overline{L}]\ , \qquad (1.1)$$

where

$$Nu_a = \bar{h}\, a/k \ ,$$

$$Gr_a = g\rho^2 \beta\, \Delta T\, a^3/\mu^2 \ ,$$

$$Pr = \mu C_p/k \ ,$$

$$\bar{L} = a/b \ .$$

The dimensionless parameters given above are the Nusselt number, Nu_a, Grashof number, Gr_a, Prandtl number, Pr, and a ratio of lengths, $\bar{L}$. These parameters adequately characterize the geometry under investigation.

At the present time there is only a limited amount of information available concerning natural convection heat transfer within finite enclosures. The case of an inner body within a spherical enclosure was first studied experimentally in 1964 by Bishop [1]. In his investigation, a concentrically located inner sphere was used for the inner body and air was employed as the gap fluid. Both spheres were maintained isothermal. Four different inner spheres were used yielding diameter ratios of 1.25, 1.67, 2.00 and 2.50. An empirical equation for the heat transfer was presented for each inner sphere used. The following equation was determined for all of the experimental data.

$$Nu_L = 0.332\, Gr_L^{0.270}\, (L/2r_i)^{0.520} \ . \qquad (1.2)$$

The above relationship fitted the data to within -12.7 per cent and +14.6 per cent, subject to the conditions:

$$Pr = 0.7 ,$$

$$0.333 \leq L/2r_i \leq 0.750,$$

$$2.0\text{x}10^5 \leq Gr_L \leq 3.6\text{x}10^5 .$$

All fluid properties were evaluated at a volumetric-mean temperature defined as

$$T_m = [(r_a^3 - r_i^3)\, T_i + (r_o^3 - r_a^3)\, T_o]/(r_o^3 - r_i^3) . \qquad (1.3)$$

Bishop also obtained data describing the temperature profiles existing at selected locations within the test gap. These were presented in conjunction with photographic studies in order to depict qualitative results with respect to the flow field which existed in the natural convective environment under investigation.

Beckmann [3] first utilized an effective conductivity in correlating natural convection heat transfer. Physically the effective conductivity represents the thermal conductivity a fluid would have to have in order to transfer the same amount of energy, by pure conduction, as actually is transferred by conduction and convection combined. Its definition -- obtained from the conduction solution of the particular geometry under investigation -- for concentric spheres is

$$k_{eff} = q_c (r_o - r_i)/4\pi \Delta T r_o r_i . \qquad (1.4)$$

Obviously the ratio k_{eff}/k has a lower limit of 1.0 which would correspond to a system transferring heat by conduction only.

Utilizing the conduction solution between concentric spheres, Bishop, Mack, and Scanlan [2] showed that a modified Nusselt number could be related to the ratio of k_{eff}/k. This relationship is given by

$$Nu^* = Nu_L (r_i/r_o) = k_{eff}/k . \qquad (1.5)$$

By employing the ratio k_{eff}/k in correlating the data, a geometric effect is included in the definition of the modified Nusselt number in an implicit manner.

Referencing the data obtained by Bishop [1], Bishop, et al [2] obtained a simplified empirical correlation using k_{eff}/k as the dependent variable. The equation,

$$k_{eff}/k = 0.106\ Gr_L^{0.276} , \qquad (1.6)$$

correlated the data within the limits of -13.4 per cent and +15.5 per cent. The conditions specified for the range of applicability of equation (1.2) are imposed upon this expression as well.

Scanlan, Bishop, and Powe [4] extended the work of Bishop [1] by utilizing water and two silicone oils as test fluids to yield the following ranges of the important parameters:

$$0.7 \leq Pr \leq 4148. ,$$

$$0.09 \leq L/r_i \leq 1.81 ,$$

$$1.2 \times 10^2 \leq Ra_L \leq 1.1 \times 10^9 .$$

Correlating in terms of the modified Nusselt number, the empirical relation obtained subject to the above conditions was

$$Nu^* = 0.202 \, (Ra_L)^{0.228} \, (L/r_i)^{0.252} \, Pr^{0.029} . \qquad (1.7)$$

The average per cent deviation of the data was 13.7 per cent.

The power of the Prandtl number appearing in equation (1.6) indicates only a slight effect of this parameter on the heat transfer results. Also, since the exponents on Ra_L and L/r_i are very nearly equal, Scanlan, et al [4] defined an adjusted Rayleigh number as

$$Ra^* = Ra_L \, (L/r_i) . \qquad (1.8)$$

The data were then correlated in the following form:

$$k_{eff}/k = 0.228 \, (Ra^*)^{0.226} . \qquad (1.9)$$

The average per cent deviation of the data from the prediction of this expression was 15.6 per cent. Although this is larger then that of equation (1.6), this form is more desirable in that it contains fewer parameters and empirical constants.

Temperature profiles were obtained for selected temperature differences impressed across the gap for each test fluid. The same trends as noted by Bishop, et al [2] were observed. In addition, the Prandtl number effect on the temperature profiles was analyzed.

The most recent investigation is that of Weber [5]. The effect of eccentricity of the two spheres was investigated, as well as the effect of changing the geometry of the inner body by using a vertical cylinder with hemispherical ends. Eccentricity is defined as a vertical displacement of the geometric center of the inner body relative to the geometric center of the enclosing sphere.

Eccentricities of $\pm$ 0.25L, $\pm$ 0.50L, and $\pm$ 0.75L, where L represents the gap width defined by $(r_o - r_i)$, were used in the investigation for each inner sphere tested. A negative eccentricity was found to enhance the convective activity and a positive eccentricity was found to have just the opposite effect.

The heat transfer data for the eccentric case were correlated using a conformal mapping technique [6] involving a geometric transformation. By utilizing this technique, a relationship was developed which also predicted the concentric data obtained by Scanlan, et al [4]. The resulting expression was

$$k_{eff}/k = 0.231\ (Ra^*)^{0.225}\ , \qquad (1.10)$$

subject to the conditions

$$0.7 \leq Pr \leq 4148. ,$$

$$1.5 \times 10^2 \leq Ra^* \leq 9.0 \times 10^8 ,$$

$$0.09 \leq L/r_i \leq 1.18 .$$

The inner radius corresponding to the mapped concentric sphere was used in defining all pertinent heat transfer parameters.

In working with the cylinder-sphere geometry, data were obtained using water as the test fluid. The height of the vertical section and the radius of the cylinder were varied in order to describe actual geometric effects on the convective heat transfer.

To maintain a certain degree of continuity in defining the pertinent heat transfer parameters, the radius of the cylinder was used in place of an inner sphere radius. Correlation of the data yielded the following equation:

$$Nu^* = 0.234 \, (Ra_L)^{0.261} \, (H/2r_i)^{-0.209} \, (L/r_i)^{0.466} , \qquad (1.11)$$

for

$$1.14 \leq H/2r_i \leq 2.0 ,$$

$$3.2 \times 10^4 \leq Ra_L \leq 2.7 \times 10^8 .$$

In equation (1.11), H represents the total height of the cylinder. Thus the ratio $H/2r_i$ has a lower limit of 1.0 corresponding to the

sphere-sphere case.

As in the previous studies, temperature profiles were obtained and these enabled deductions regarding the flow field to be made.

Since water was the only test fluid employed for the cylinder investigation, there exists a need to extend these results by using additional fluids. In the current study, two silicone oils will be used in conjunction with the cylindrical inner body to investigate the effect, if any, the Prandtl number has on the convective heat transfer. Sufficient data were obtained by Weber [5] to depict the geometric effects.

As noted in the previous discussion, the cylindrical inner body produced results which varied significantly from the sphere data. This is what would be physically expected. However, there is a certain degree of similarity between the two geometries. Therefore, to more adequately describe the natural convection phenomena occurring within a spherical enclosure, the effects of a cube located concentrically within the enclosing sphere for several test fluids will also be investigated.

CHAPTER II

EXPERIMENTAL APPARATUS AND PROCEDURE

EXPERIMENTAL APPARATUS

The experimental apparatus, shown in Figure 2.1, consisted of an inner body located concentrically within a sphere having an inner diameter of 9.828 inches and a wall thickness of 0.125 inches. The sphere was formed from two stainless steel hemispheres joined together by an external flange to permit disassembly and removal of the inner body. An O-ring was placed in the parting plane for sealing purposes. The lower hemisphere was mounted to an enclosing spherical water jacket by using a metal spacer.

The spherical water jacket consisted of two steel hemispheres, the lower being attached to a tubular support frame mounted on a metal table. The hemispheres were united using a flexible band surrounding external flanges attached to the hemispheres. The inner diameter of this sphere was approximately 14 inches.

A stainless steel tube of 0.25 inch inside diameter was installed through the apparatus, extending from the inner surface of the enclosing sphere to the outside of the water jacket. The tube, which was located near the lower extreme of the apparatus, served as a fill port for injecting the test fluid into the gap.

The inner bodies were of cylindrical and cubical geometry. The

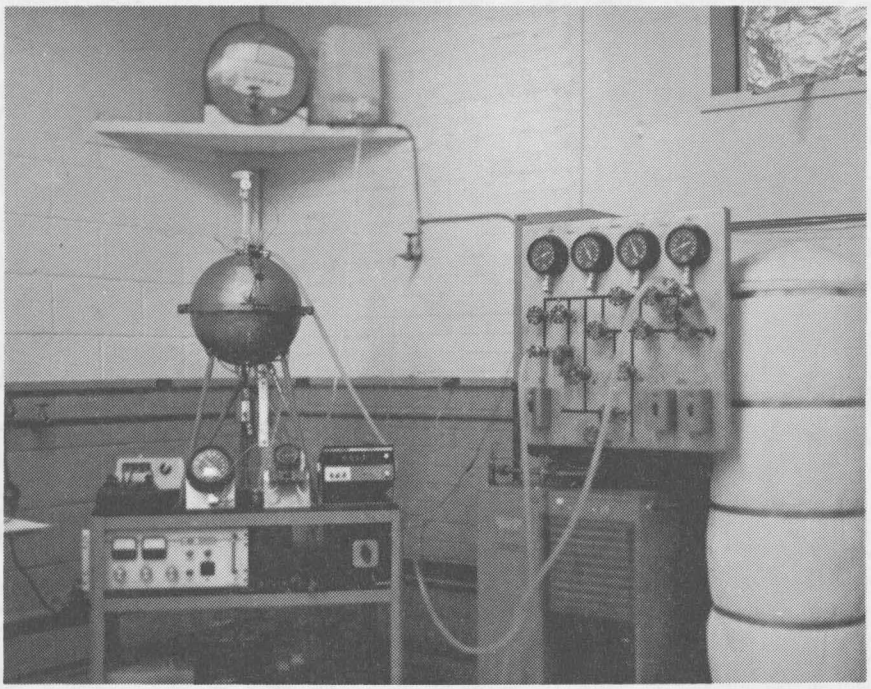

Figure 2.1. Heat transfer apparatus.

cylindrical bodies, made of 0.065 inch thick copper, were formed from a cylinder having hemispherical ends. The cubes were fabricated out of an aluminum alloy suitable for welding. Each inner body was mounted on a stainless steel stem having an inside diameter of 0.37 inches and an outer diameter of 0.50 inches. The outer surface of the stem was insulated to reduce the amount of heat loss from the system.

A uniform inner body temperature was maintained by condensing Freon-11 on the inner surface of the test geometry. Heaters mounted to the stem extended into the inner body. Electrical disk heaters were used with the cylindrical geometry and cartridge heaters for the cubical geometry. The size and number of heaters used was dependent upon inner body size. Figures 2.2 and 2.3 illustrate typical arrangements of the heaters within the bodies prior to their final assembly. Saturation conditions of the Freon-11 could be varied by regulating the power supplied to the heaters. Thus, the inner body temperature could be varied over a desired range of values.

Copper-constantan thermocouples were used to monitor all temperatures. In the case of the cylinders they were located in the joining seams. For the cubical geometries a small hole was drilled through the cube wall at a selected location, and a Shell Epon resin was used to affix the thermocouple to the outer surface. All power and thermocouple leads were passed down through the supporting stem.

The support stem passed through the enclosing sphere and water

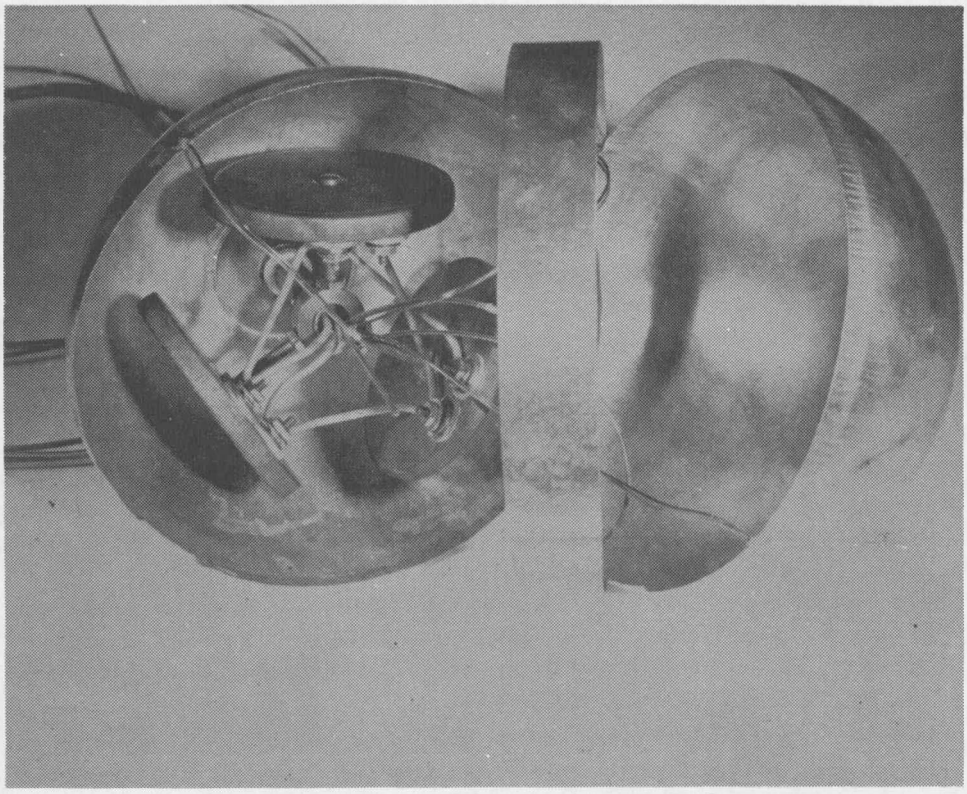

Figure 2.2. Interior of cylinder body.

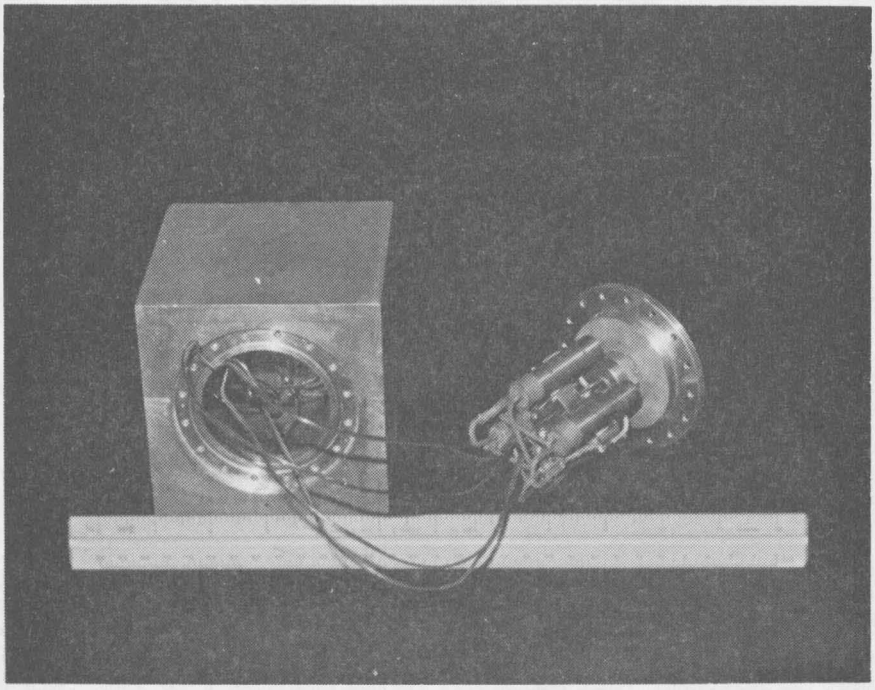

Figure 2.3. Interior of cube body.

jacket through holes sealed with O-rings and was attached to a stainless steel reservoir. The reservoir rested on a threaded rod used to position the inner body to any desired vertical location within the enclosing sphere. All thermocouple and power leads were withdrawn from the reservoir and channeled to the appropriate instrumentation. A needle indicator attached to the reservoir traversed along a scale which indicated relative positioning of the inner body.

A hollow stainless steel tube of approximately 0.065 inch outer diameter was mounted to the inside of the support stem and extended to the upper region of the inner body. The tube, emerging from the reservoir, was connected to a pressure gage to monitor the pressure within the body during experimental runs. In addition, the tube served as a vent line during Freon charging.

A closed water cooling system was employed to maintain the sphere enclosing the inner body at a constant temperature. The cooling system consisted of an insulated storage tank, a pump, and two chillers. The chilled water was introduced at the bottom of the spherical water jacket through a manifold system and withdrawn in a similar manner from the top.

Thermocouple probes used for obtaining temperature profiles were constructed by passing copper-constantan leads through stainless steel tubes of 0.065 inch outside diameter. Epoxy cement was used to firmly attach the thermocouple to the tubing end. Appropriate fittings

equipped with O-ring seals were mounted and aligned on the external surfaces of the water jacket and enclosing sphere to allow the inserted probes to reach the surface of the inner body. A vernier caliper, graduated to 0.001 inch, was modified to permit attachments to the fittings on the water jacket for positioning the probes within the test gap. A total of five probes spaced at 40° increments were used, with the upward vertical axis of the apparatus corresponding to the 0° position.

EXPERIMENTAL PROCEDURE

The inner body to be investigated was selected and mounted in the heat transfer apparatus. The thermocouple and power leads, in addition to the vent tube, exiting from the stainless steel reservoir were connected to the appropriate instrumentation. The upper hemispheres of the enclosing sphere and water jacket were fastened in place using flexible metal bands.

The inner body was then charged with Freon-11 using a gravity feed system. The Freon entered the system through the stainless steel reservoir, flowing up the stem into the inner body. A valve located on the line leading from the pressure gage was opened to allow the entrained air within the inner body to escape. When a stream of Freon was visually seen flowing through the vent line, the valve on the line leading from the Freon reservoir was closed. A predetermined volume of Freon was then drained from the inner body by means of a

valve mounted on the stainless steel reservoir. The desired volume being removed, all valves were closed.

All thermocouple probes were installed with the exception of the one at the 0° position. Here a stainless steel tube, extending just into the enclosing sphere, was inserted. The desired test fluid was injected into the gap utilizing gravity as the driving force. When the fluid was visually seen exiting through the stainless steel tube, the uppermost probe was installed.

With the cooling system finally being connected to the water jacket, the experimental apparatus was ready for operation.

When testing the cylindrical inner bodies, the experimental fluids used were 20 cs and 350 cs silicone oils. The silicone oils are a Dow Corning 200 fluid with the 20 cs and 350 cs representing the kinematic viscosity of the fluid at 25°C. For the cubical geometry, air and the two silicone fluids were employed.

Since the heat transferred by natural convection was desired, a means of predicting all heat losses from the system was necessary. The heat losses consisted of conduction down the support stem and radiation between the inner body and the enclosing sphere when air was being used as the test fluid.

Experimental runs involving the silicone oils required accounting for stem losses only since the fluids are opaque to radiation. This was predicted by applying the one dimensional, steady state conduc-

tion equation

$$q_{cond} = -k\, A(\Delta T/\Delta x) \,. \qquad (2.1)$$

The procedure described by Bishop [1] was used to predict the heat losses when air was used as the working medium. A calibration curve was obtained for each cubical inner body tested in the following manner. A vacuum of 10-40 microns was created and maintained in the gap. This effectively forces the convection of energy in the gap to be negligible in comparison with conduction down the stem and with radiation. Thus, the energy supplied to the heaters essentially becomes equal to the system's heat losses. The enclosing sphere temperature, assumed to be the average of the inlet and outlet cooling water temperatures, was maintained at a constant value throughout the calibration procedure. This same temperature was also maintained during all test runs using air as the working fluid.

The apparatus was allowed to operate for approximately 15 - 24 hours for each data point to insure that steady state conditions had been reached, and at that time the following data were recorded:

(1) Freon-system pressure,

(2) Pressure in the gap,

(3) Temperature of cooling water,

(4) Temperature of inner body,

(5) Heater voltage and current,

(6) Run number.

Sufficient data were obtained to depict the variation of the heat loss over the anticipated inner body temperature range to be covered during experimental runs. Figure 2.4 contains the curve generated for each cube. As indicated, a linear relation was generally noted between the cube temperature and heat loss -- indicating conduction losses were predominant over radiation losses. Thus, an equation of the form

$$q_L = C_1 T_i + C_2 \,, \tag{2.2}$$

was determined for each cube using a least squares technique. The equations obtained are listed on the figure.

During experimental runs, the data, as listed above with the exception of gap pressure, were recorded. Table 2.1 contains the description of each cylindrical body tested as well as a listing of test fluids for which data were obtained. Three cubical bodies, having lengths of 2.515, 4.190, and 4.945 inches, were investigated.

Temperature profiles within the gap were obtained for each test fluid and inner body studied. The vernier caliper was attached at the desired probe location. The probe was introduced into the gap until contact with the inner body was established. The probe was then withdrawn incrementally. The temperature corresponding to the relative gap distance was recorded for each increment tested. Heat transfer

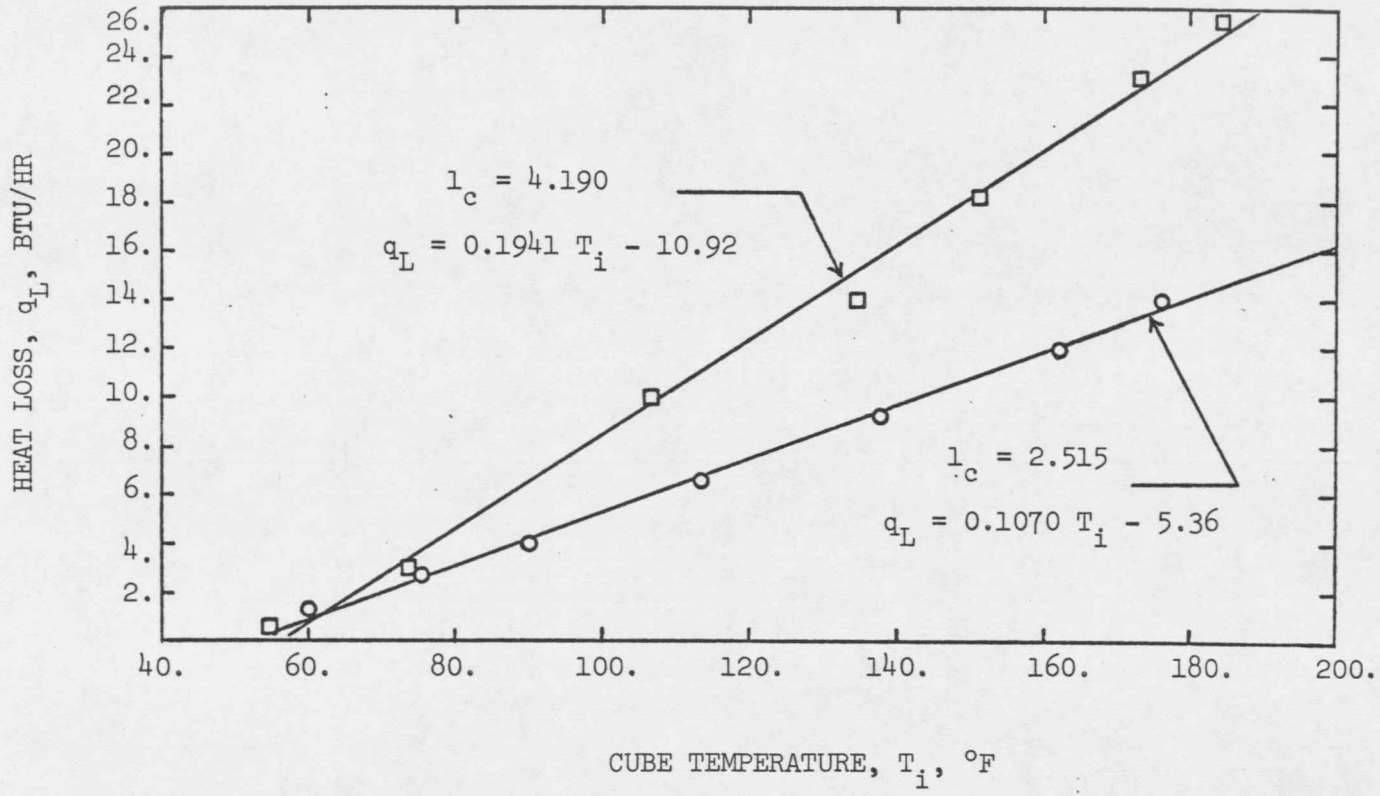

Figure 2.4. Calibration curves for determining heat transfer loss for $T_o \sim 41°F$.

TABLE 2.1

DIMENSIONS OF CYLINDER BODIES AND TEST FLUIDS
USED WITH EACH BODY

Diameter D (IN)	Overall Length H (IN)	Water[1]	Silicone 20 cs	Silicone 350 cs
4.50	6.75	x		
	8.75		x	
5.50	7.125	x	x	x
	8.812	x	x	x
7.00	8.00	x		
	8.875	x		
9.0	9.328	x		

[1] Data were referenced from [5].

data, as discussed previously, were taken upon completion of each of the runs for five probes to insure that the system had remained in equilibrium during the data taking process. Flow symmetry was assumed to exist within the gap for the cylinder-sphere geometry for steady flow patterns. Thus, only one complete profile, as described above, was needed. For the cubical inner body, traverses were made in two vertical, central planes -- one perpendicular to a cube face and the other through a vertical edge of the cube. Although this does not fully depict the flow field, trends can be determined from these data.

A computer program was written for the XDS Sigma 7 digital computer to convert the experimental data into the desired form. The program used for the cube-sphere geometry is listed in Appendix I. Appropriate modifications were made in defining the pertinent parameters when reducing the cylinder data.

The amount of heat transferred by natural convection was determined by the use of the equation

$$q_c = 3.413\ VI - q_L \ . \tag{2.3}$$

An average heat transfer coefficient was then defined as

$$\overline{h} = q_c / A_s (T_i - T_o) \ , \tag{2.4}$$

where A_s represents the surface area of the inner body.

An arithmetic-mean temperature, defined below, was used to eval-

uate all fluid properties for this investigation.

$$T_{am} = (T_i + T_o)/2 \ . \qquad (2.5)$$

Function sub-programs were utilized to convert the millivolt readings generated from the thermocouples to temperatures and to yield all required fluid properties as a function of temperature. A listing is provided in Appendix I.

CHAPTER III

CYLINDER RESULTS

HEAT TRANSFER DATA

The cylinder-sphere studies performed by Weber [5] employed water as the test fluid. The current investigation extended these data by utilizing additional test fluids to examine the effect of Prandtl number on the convective heat transfer rate. The raw data obtained by Weber are referenced and included in the graphical representation and heat transfer correlations to be presented.

The effect of a change in the length of the cylinder for a constant cylinder diameter is illustrated in Figures 3.1, 3.2, and 3.3 for water, silicone 20, and silicone 350 fluids respectively. This effect is presented graphically by plotting Nusselt number versus Grashof number for a 5.5 inch diameter cylinder having overall lengths of 7.125 and 8.812 inches. As indicated in Figure 3.1, this effect is quite noticeable for water, the longer length resulting in a lower Nusselt number. The more viscous fluids tend to damp out the geometric effect as indicated in Figures 3.2 and 3.3. Weber postulated that the effect was greater for the larger diameter ratios with no noticeable difference for values of D_o/D_i less than 1.4.

Figure 3.4 contains all of the cylinder heat transfer data. The results were plotted using equations (1.5) and (1.8) for the modified

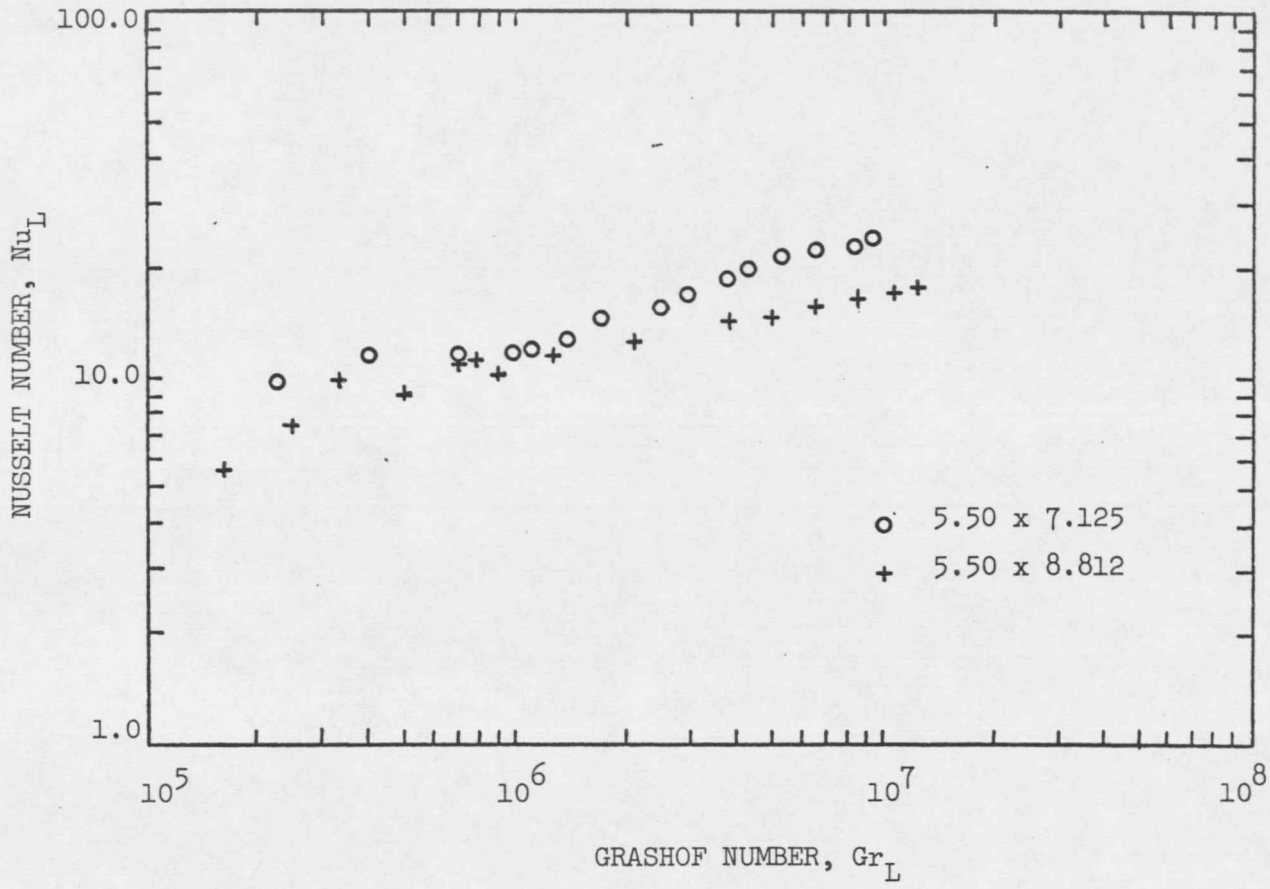

Figure 3.1. Heat transfer data for the 5.50 inch diameter cylinders and water.

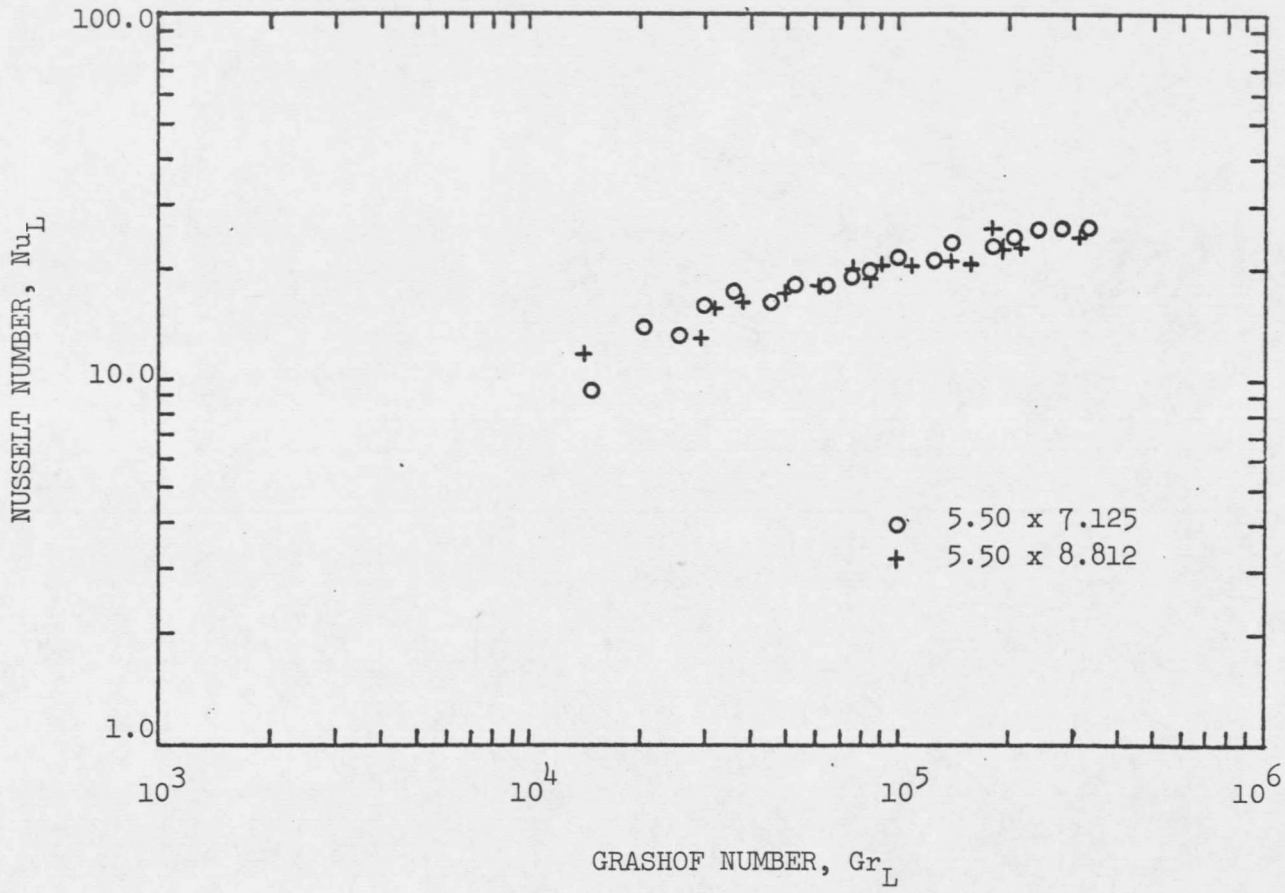

Figure 3.2. Heat transfer data for the 5.50 inch diameter cylinders and silicone 20 cs.

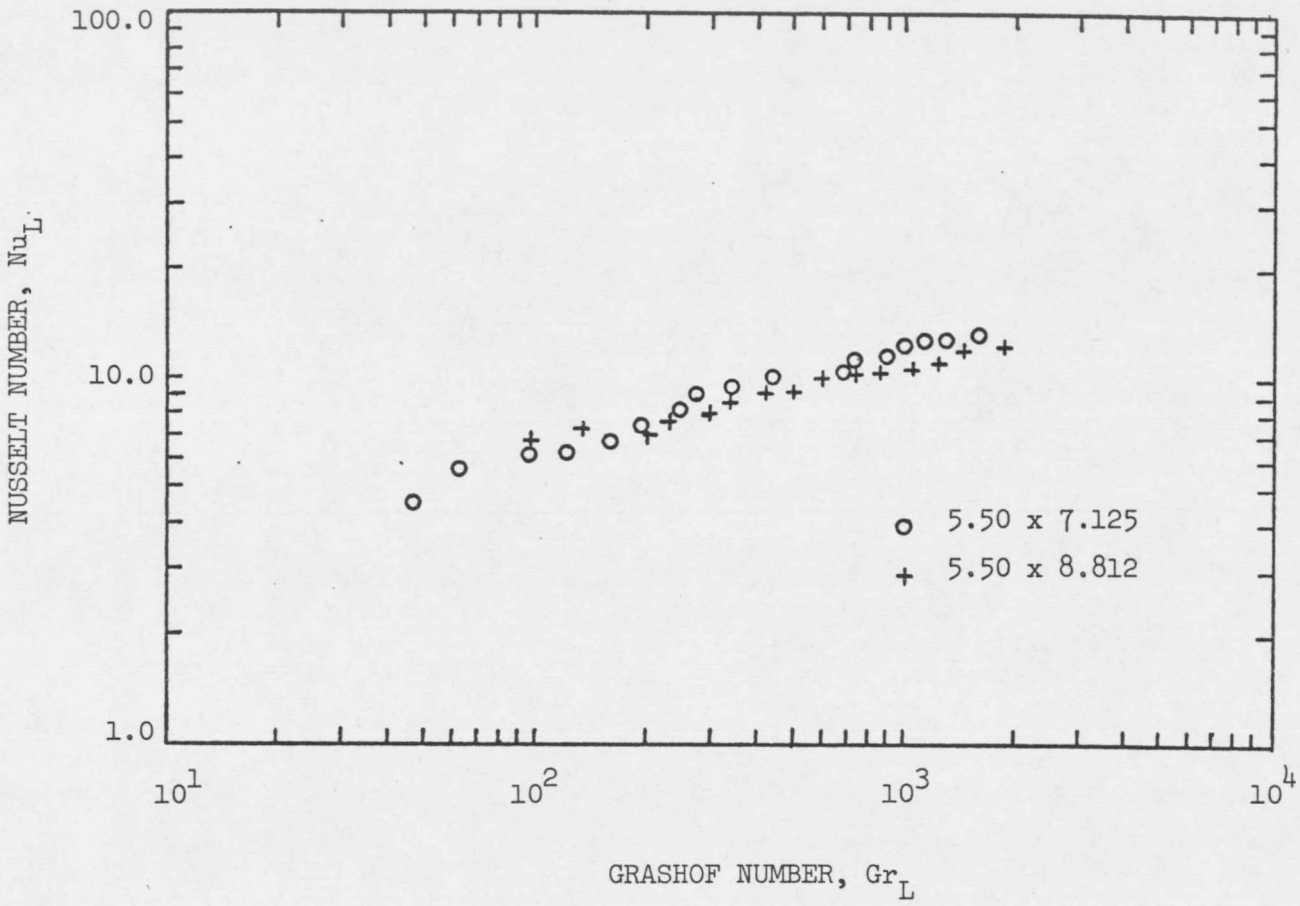

Figure 3.3. Heat transfer data for the 5.50 inch diameter cylinders and silicone 350 cs.

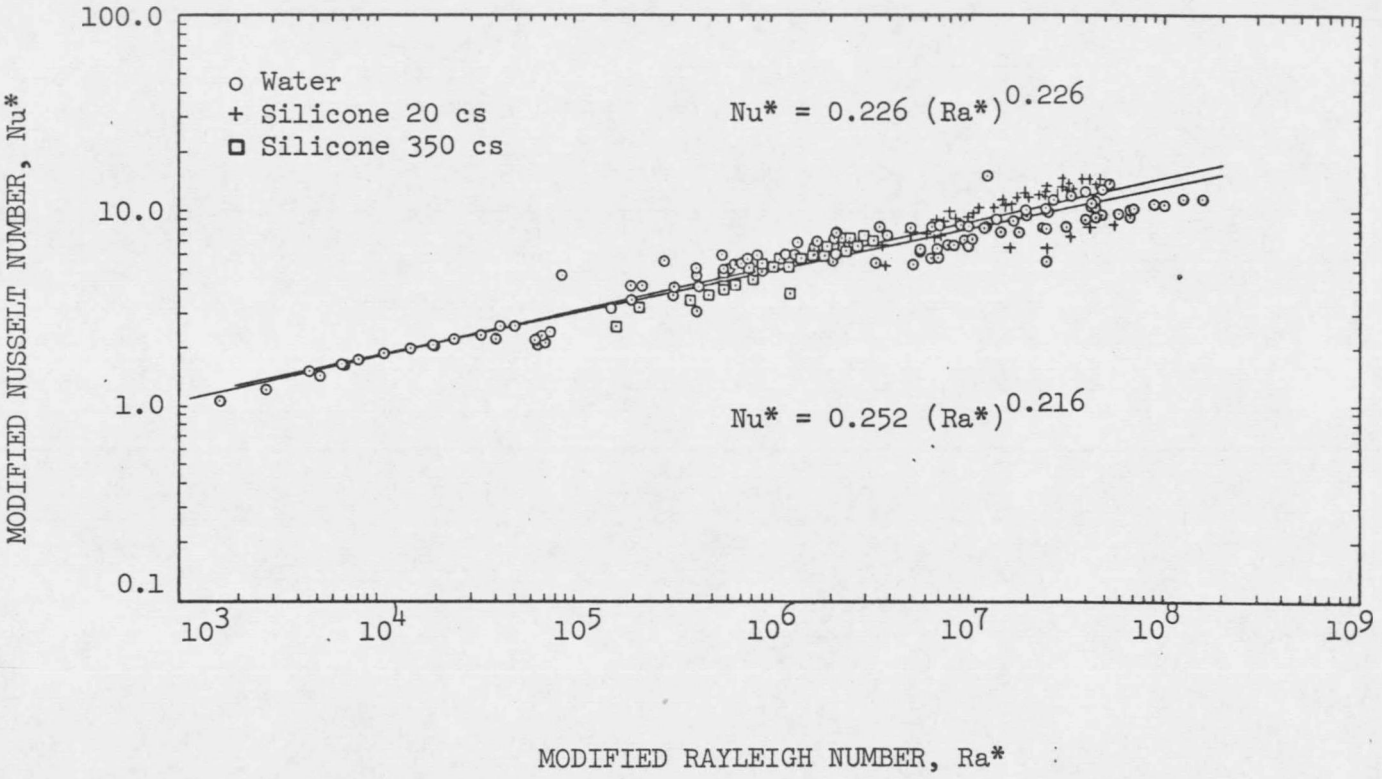

Figure 3.4. Heat transfer results for all cylinders and fluids.

Nusselt and Rayleigh numbers, respectively. The radius of the cylinder was used as an inner radius in these definitions. It is apparent from this figure that there exists more scatter of the data for water than for the silicone fluids. Investigators utilizing water as a test fluid have generally noted this trend in previous investigations with no physical explanation as to why this is the case. In addition, it appears that the heat transfer data may be correlated in terms of the adjusted Nusselt number as a function of the modified Rayleigh number only.

A dimensional analysis of the system under investigation indicates that the heat transfer may be correlated in the form

$$Nu_a = F[Ra_a, Pr, H/2r_i, L/r_i] . \tag{3.1}$$

Using a least squares technique as described in [7], an equation of the form

$$Nu_L = C_1 Ra^{C_2} Pr^{C_3} (H/2r_i)^{C_4} (L/r_i)^{C_5} , \tag{3.2}$$

was used in an attempt to correlate the data. The resulting expression is given by

$$Nu_L = 0.181 Ra_L^{0.280} Pr^{0.042} (H/2r_i)^{-0.711} (L/r_i)^{0.397} , \tag{3.3}$$

and is subject to the limits

$$1.8x10^4 \leq Ra_L \leq 1.4x10^8 ,$$

$$6.8 \leq Pr \leq 4302. ,$$

$$1.036 \leq H/2r_i \leq 1.944 .$$

Equation (3.3) was characterized by an average per cent deviation of 9.0, with 91.7 per cent of the data falling within $\pm$ 20 per cent of its prediction. Although the exponent of the Prandtl number is small, it was found that the deletion of this parameter from the equation significantly effects the results. Weber [5] found the above form to best represent the heat transfer data for water with the omission of the Prandtl number since it had a negligible effect. This is physically sound in that only one fluid was represented. Figure 3.5 illustrates the Prandtl number effect on the heat transfer results. Nusselt number is plotted versus Rayleigh number for the three test fluids and one cylinder size. Since there is a noticeable separation in the plots of each fluid, a Prandtl number effect is indicated. Of interest to note is the closeness to which the cylinder data fall relative to the equations obtained in [4] for the sphere studies, as represented by the solid lines.

Since it was desired to maintain a certain degree of continuity between these data and previous results involving convective heat transfer within a spherical enclosure, the Nusselt and Rayleigh numbers were modified using equations (1.5) and (1.8). An equation of the form

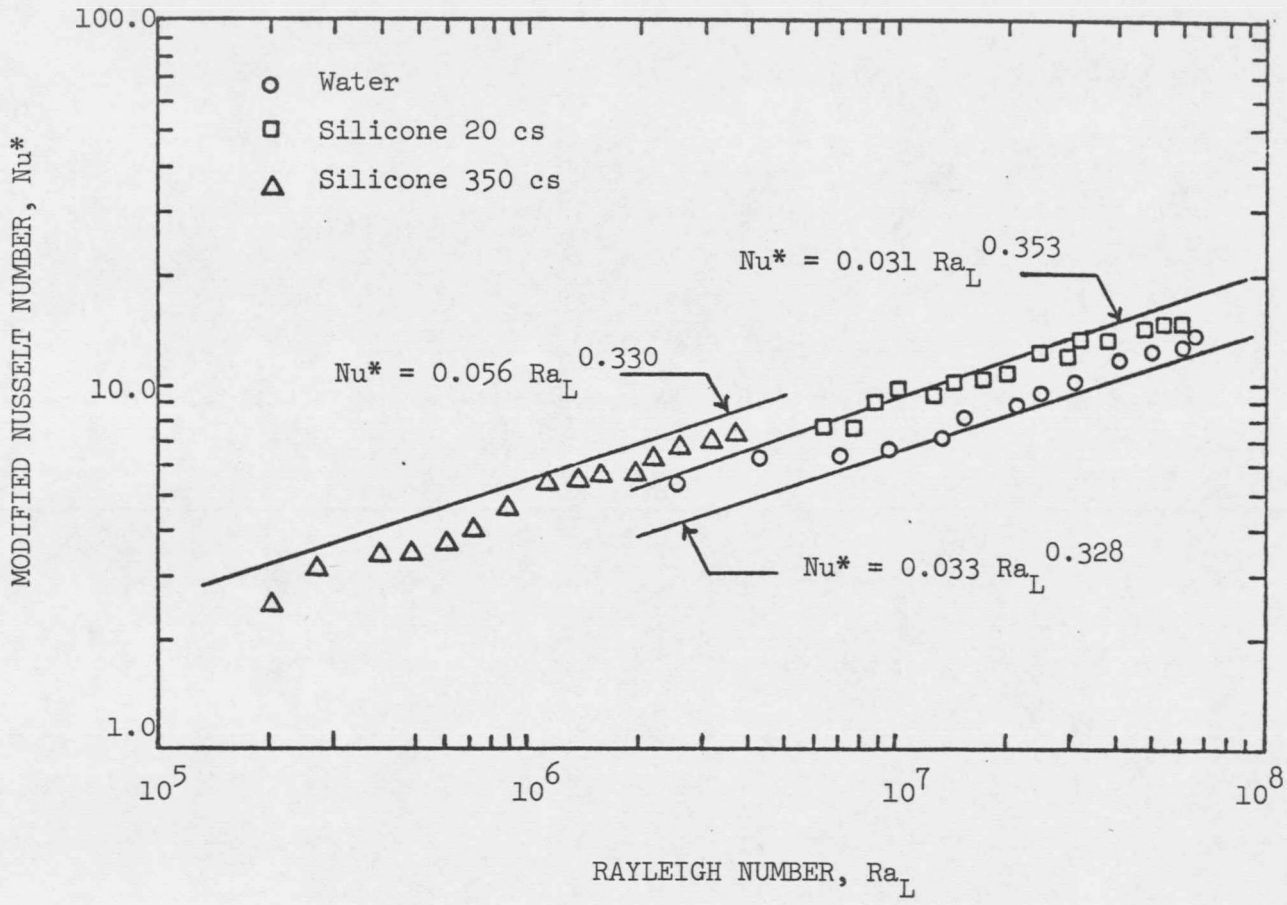

Figure 3.5. Heat transfer results for 5.50 x 7.125 inch cylinder and all fluids.

$$Nu^* = C_1 (Ra^*)^{C_2} (H/2r_i)^{C_3} Pr^{C_4} , \qquad (3.4)$$

was then used to correlate the data with the following result:

$$Nu^* = 0.164 (Ra^*)^{0.257} (H/2r_i)^{-1.02} Pr^{0.035} . \qquad (3.5)$$

This expression had an average per cent deviation of 10.7 with 86.8 per cent of the data falling within $\pm$ 20 per cent of its prediction.

A primary goal in this study was to correlate the cylinder data with existing empirical relationships for concentric spheres. Although in equation (3.5) the ratio $H/2r_i$ has a lower limit of 1.0, corresponding to a sphere geometry, this expression differs significantly from a similar form obtained for concentric spheres (see [4]). Using equation (1.7) as a base, the prediction

$$Nu^* = 0.202 Ra_L^{0.228-0.017h/2r_i} (L/r_i)^{0.252-0.579h/2r_i} Pr^{0.029-0.012h/2r_i} , \qquad (3.6)$$

was determined yielding an average per cent deviation of 11.8 with 88.0 per cent of the data within $\pm$ 20 per cent of the equation.

Accompanied with a slight loss in apparent accuracy, a simpler form was obtained using equation (1.9). This is given by

$$Nu^* = 0.228 (Ra^*)^{0.226-0.05h/2r_i} (H/2r_i)^{0.759} , \qquad (3.7)$$

and has an average deviation of 12.8 with 79.3 per cent of the data falling within $\pm$ 20 per cent of the equation.

Equation (1.9) is shown plotted in Figure 3.4. As clearly illustrated, the cylinder data lie extremely close to its prediction. Also plotted is the correlation

$$Nu^* = 0.252\ (Ra^*)^{0.216}\ , \qquad (3.8)$$

which was obtained for all the cylinder data. An error analysis yielded an average deviation of 14.6 per cent which is comparable to the 15.6 per cent figure obtained for the sphere-sphere studies. It should be noted that the fluid properties in the sphere investigation were evaluated at a volumetric weighted mean temperature and those for the cylinder at an arithmetic mean. Also the use of the modified Nusselt and Rayleigh numbers is arbitrary for the cylinder case.

TEMPERATURE DISTRIBUTION

The experimentally determined temperature profiles are presented in graphical form using a dimensionless radius ratio defined as

$$\overline{R} = (r - r_\theta)/(r_o - r_\theta)\ , \qquad (3.9)$$

and the dimensionless temperature ratio

$$\overline{T} = (T - T_o)/(T_i - T_o)\ . \qquad (3.10)$$

Thus, both ratios vary from zero to one.

The parameter r_θ , as used in $\bar{R}$, is a function of angular position and therefore distorts to some degree the profile curves relative to each other. However, this is perhaps the most convenient representation of the data.

Temperature profiles, in general, exhibited the same trends as noted in previous investigations [1,2,4,5]. Therefore only representative results will be presented herein.

As illustrated in Figure 3.6, there are five characteristic regions which are described below:

(1) a relatively large temperature drop occurring next to the surface of the inner body which is indicative of a relatively high velocity flow and a large radial transport of heat at the inner boundary;

(2) a transition region from a high velocity to a low velocity moving fluid;

(3) a region of small change in temperature gradient and slow moving fluid;

(4) a transition region connecting slow to high velocity fluid motion; and

(5) a relatively steep temperature gradient approaching the surface of the enclosing sphere.

The transition regions are seen to extend into the gap a consider-

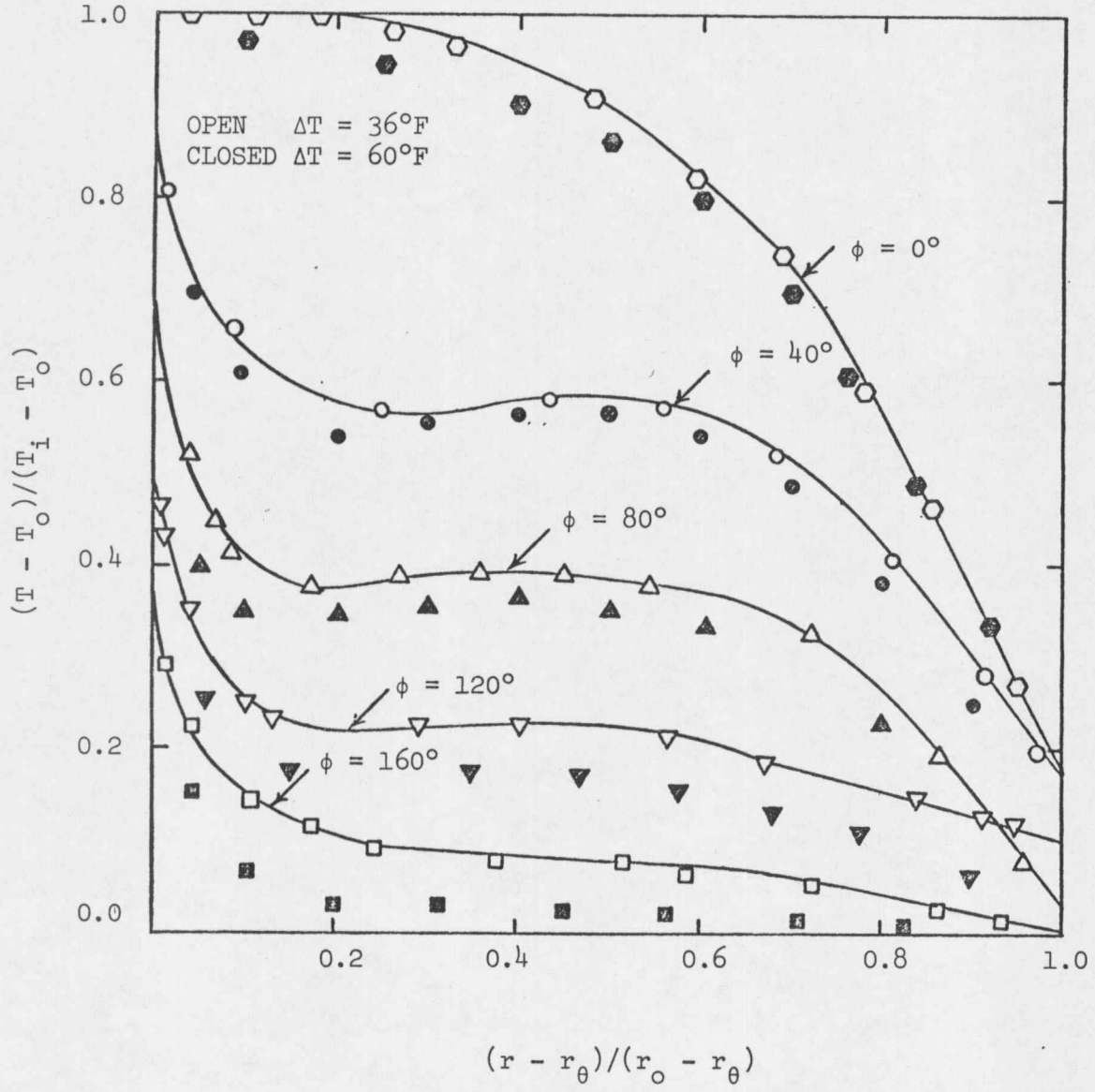

Figure 3.6. Temperature profile for the 5.50 x 7.125 inch cylinder and silicone 350 cs.

able distance. This is due to the viscous motion of the test fluid. The more viscous the fluid, the further the transition regions extend into the gap.

Another trend apparent in Figure 3.6 is the general lack of dependence of the shape of the profile with respect to the impressed temperature potential across the gap. This is consistent with past studies and was observed for both silicone fluids and for all cylinders tested. Figure 3.7, a typical result for the silicone 20 fluid, depicts the general ordering of the probes relative to each other. This figure is indicative of a monocellular flow existing within the test gap. The temperature variation for the 160° position illustrates a phenomenon inherent to all profiles. This region is characterized by a slow moving fluid with the majority of heat being transferred in the region of close proximity to the inner body.

Figure 3.8 contains results which vary from the general trends previously described in that the 0° position is seen to fall between the 80° and 120° positions. This occurrence, as first observed by Bishop [1], can be explained by the presence of a multicellular flow pattern. An extensive flow visualization study performed by Yin [8], substantiated this phenomenon.

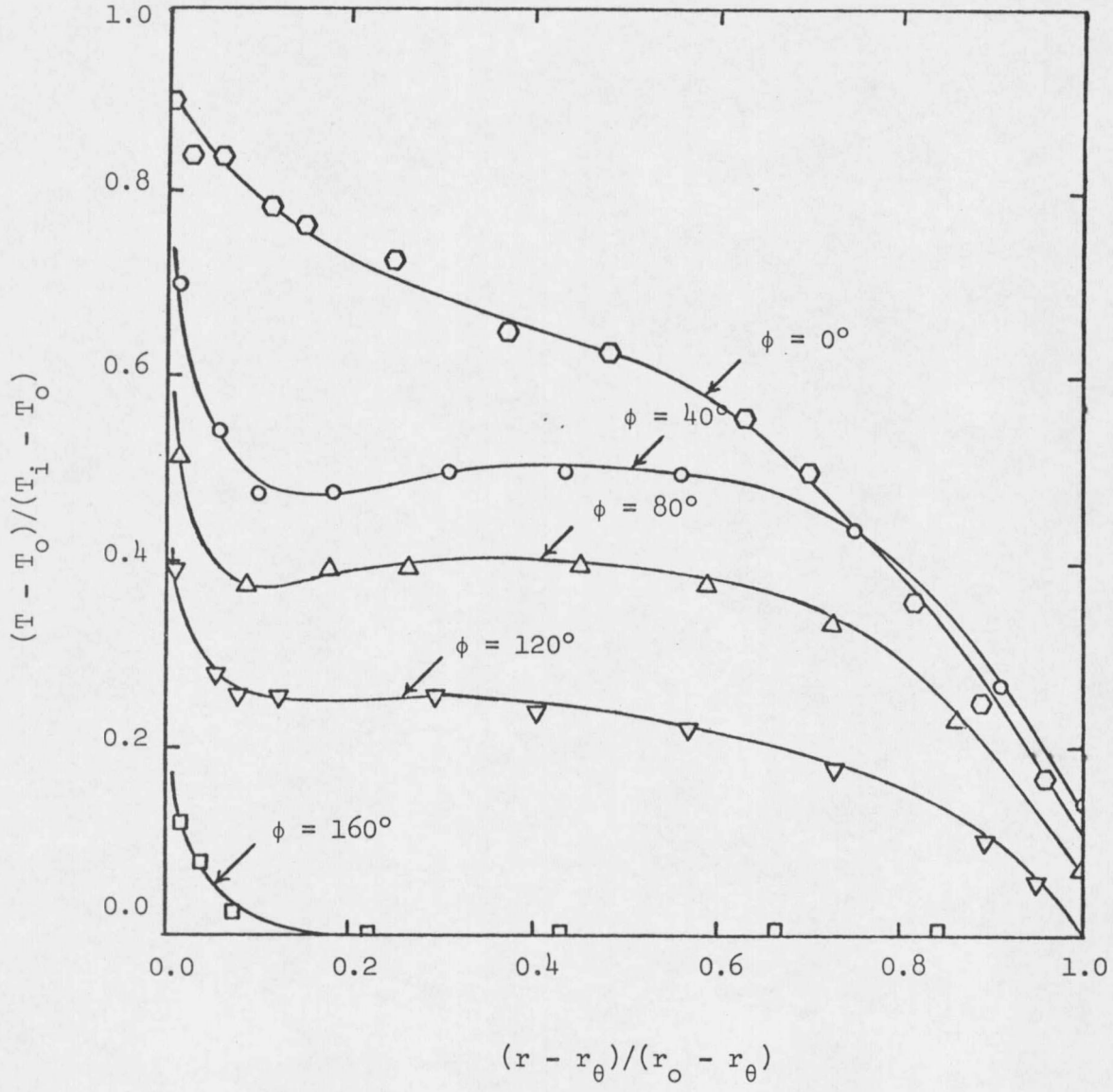

Figure 3.7. Temperature profile for the 5.50 x 7.125 inch cylinder, silicone 20 cs, and $\Delta T = 22.2°F$.

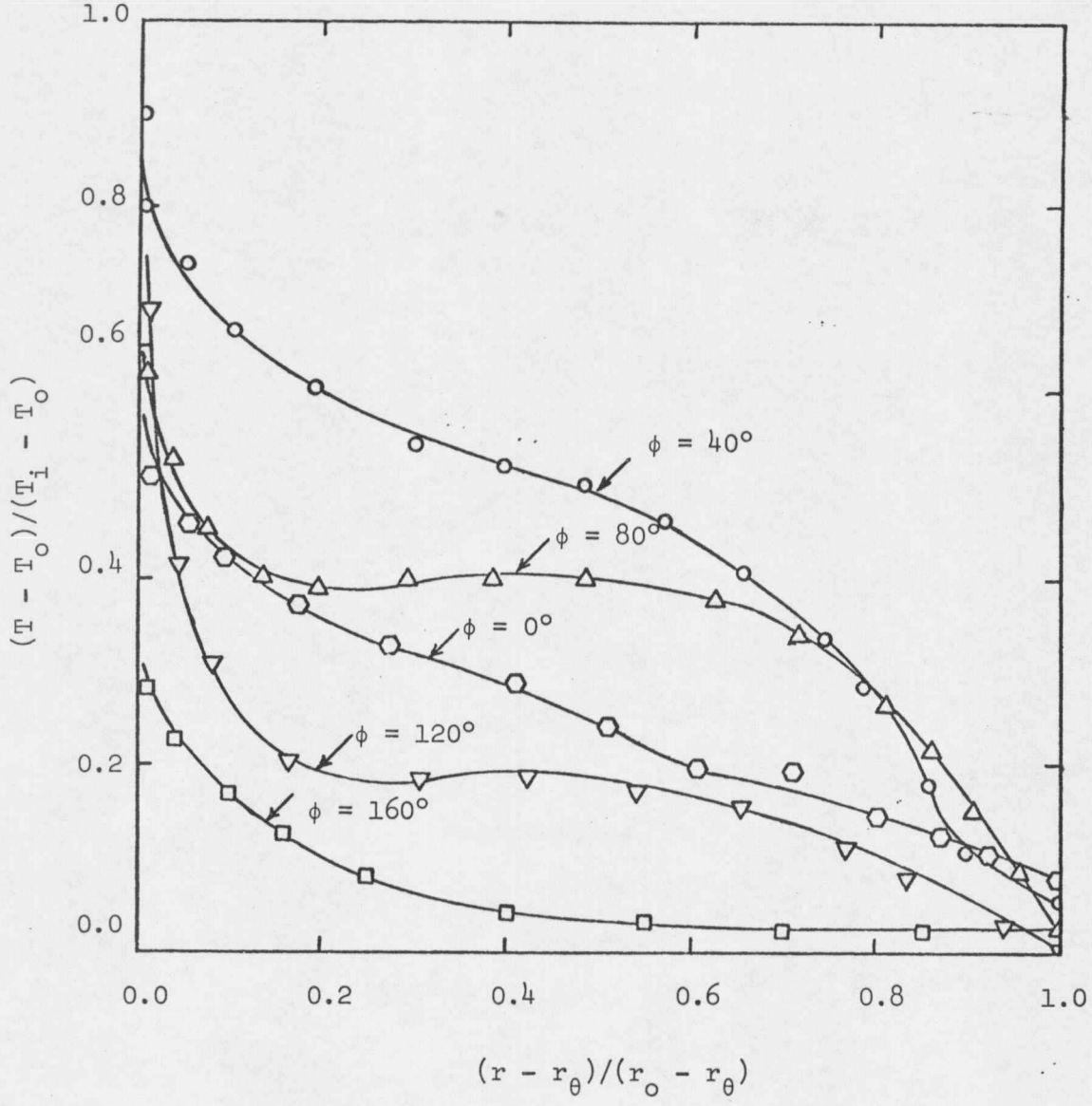

Figure 3.8. Temperature profile for the 5.50 x 8.812 inch cylinder, silicone 350 cs, and ΔT = 41.8°F.

CHAPTER IV

CUBE RESULTS

HEAT TRANSFER DATA

The characteristic length dimension used in defining all pertinent heat transfer parameters for the cube-sphere investigation was half the length of a side. Utilizing this parameter allowed reasonable representation of the heat transfer results.

Figures 4.1, 4.2, and 4.3 contain the raw heat transfer data plotted as Nusselt number versus Grashof number for air, silicone 20 and silicone 350 fluids, respectively. These figures illustrate the effect of cube size on the Nusselt number. As indicated on all three plots, a larger cube size yielded a lower value of the Nusselt number.

Figure 4.4 is a graphical representation of the cube data in terms of Nusselt number versus Rayleigh number for all cube sizes and fluids investigated. This plot clearly illustrates that there exists only a very small Prandtl number effect on the heat transfer. The Prandtl number appears in the definition of the Rayleigh number to the first power. Thus, the Prandtl number is included in the data representation in an implicit manner.

An attempt was made to correlate the data using an equation of the form